The Duality Droop Control for Grid-Tied Cascaded Microinverter

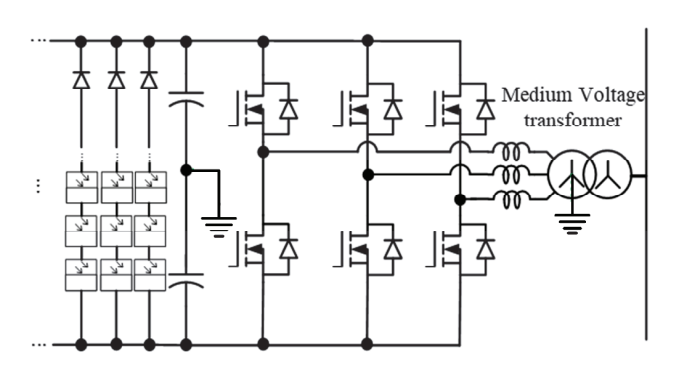
Maohang Qiu, Mengxuan Wei, Xiaoyan Liu, Dong Cao Electrical and Computer Engineering Department University of Dayton Dayton, Ohio

qium02@udayton.edu, weim06@udayton.edu, liux46@udayton.edu, dcao02@udayton.edu

Abstract— Cascaded Connected Microinverter (CCM) system takes the advantage of adapting low voltage stress submodules to build the high voltage output, which makes it easier and safer to achieve for many applications. The distribution of active and reactive power in the CCM system has always been additional communication interdependent, resulting in components in different submodules. Such communication components within different submodules can be avoided by droop control. Droop control is widely adopted in parallel inverter system, and it originates from the synchronous generator that active power is controlled by adjusting synchronous generator's frequency and reactive power is controlled by adjusting its output voltage. However, the traditional droop control is not suitable for the cascaded microinverter inverter system. Therefore, it's necessary to modify the droop control to make it suitable for Cascaded Microinverter system, and therefore a control method called inverse droop control is adopted for cascaded inverter system under island mode. However, it requires a large feeder inductor when it's grid connected since every submodule works as voltage source inverter. In this paper, a duality control method that feedbacks each submodule's active power and reactive power to adjust its inductor current amplitude and frequency respectively is proposed. Compared with traditional cascaded inverter system that's controlled by inverse droop control method, the big line frequency feeder inductor is saved.

I. INTRODUCTION

Distribute generator has been widely studied recently for new energy resources applications, such as photovoltaic(PV) panel, wind turbines, and tidal energy converter. In the medium voltage area, the typical structure of a PV power plant is shown in Fig. 1. It consists of a three-phase inverter, a three-phase medium-voltage transformer, and plenty of PV panels. This structure has been commercially used for decades and the power rating can reach to megawatt level [1]. However, the system efficiency is relatively low since only centralized maximum power point tracking (MPPT) control can be performed. Moreover, the bulky and heavy line-frequency transformer significantly increases the whole system's cost, volume, and weight [2]. To solve this issue, the microinverter has been proposed. However, traditional microinverter can only output relatively low AC voltage for residential and commercial applications. Instead, Cascaded Connected Microinverter



(CMI) can adopt low voltage submodules to achieve a high voltage output for medium voltage applications without using the bulky line-frequency transformer [3]-[5]. Therefore, both the weight and volume of the whole system can be greatly

Fig. 1 Traditional grid-tied medium voltage solar inverter system.

reduced. By replacing the submodule of CMI with a microinverter, every submodule of CMI can perform its own MPPT, which can realize relatively higher solar conversion efficiency than the typical structure does, and this structure is also called cascaded connected micro-inverter (CCM). Furthermore, with the development of wide bandgap devices, the low voltage, low conduction loss, and high switching speed Gallium Nitride(GaN) devices can be utilized to achieve extremely high power density converter design [6]-[9]. Therefore, by adopting these low voltage GaN devices for the submodule design of CCM, very high-power density inverter systems with high output voltage can be achieved.

In the CCM system, power-sharing and communication within different submodules are two hot issues that are vastly investigated. These issues could be easily solved if the CCM system is controlled in a centralized structure. The centralized structure requires a central calculation unit to burden all the calculation tasks and all submodules' ADC data should be transferred to the central unit. This central unit spreads out the PWM signals to every submodule after finishing all the calculations [10]. As a result, it is very suitable for the case that all submodules can be integrated into one PCB board in low power and low voltage applications. However, for medium voltage applications, the distance between two submodules becomes far, such a centralized control structure will be more difficult to be realized. In this case, the high-bandwidth communication system must be adopted to synchronize all

submodules' phases. For example, Reference [11] adopts a high-bandwidth interconverted communication system to transmit time-critical control signals within different submodules. Under such circumstances, the hardware cost is much higher with relatively lower robustness. To solve these issues of the central control structure, different methods have been proposed in [12], [20], which mainly focus on communication-free solutions. In general, they can be divided into two categories based on whether the droop control is adopted. The droop control method originates from the synchronous generator that active power is controlled by adjusting the synchronous generator's frequency and reactive power is controlled by adjusting its output voltage. This control method has been successfully adopted in the parallel-inverter system, where the communication among different submodules can be totally avoided. Reference [12] applies the droop control concept into CCM system so that the communication can be totally avoided, and it is also named inverse droop control. Reference [13]-[21] doesn't adopt inverse droop control to synchronize the submodules' phase, instead, each submodule directly samples the point of common coupling (PCC) voltage to synchronize its phase. Although the communication can be avoided, the measurement circuits for PCC voltage are still required for each submodule. Therefore, they are still communication-dependent systems since every submodule should obtain PCC voltage information. Generally speaking, these methods make each submodule of the cascaded microinverter system work as voltage-source inverter. As a result, the feeder inductor is required if the cascaded microinverter system is in grid-tied mode while the feeder inductor can be saved if the cascaded microinverter system works in island mode. Therefore, the cascaded microinverter system will become much more unified if the feeder inductor can be totally removed under both grid-tied and island mode.

If the feeder is removed, then all the submodules should work as current-source mode which is shown in the Fig.1(A). Moreover, all submodules should keep the same active and reactive power distribution. According to the traditional droop control method for parallel microinverter system, the duality droop control method for cascaded microinverter can be derived. Compared with the traditional droop control method that sets the submodule's output voltage as control goal, the duality droop control sets the submodule' s output current as control goal. Section II derives the duality droop control method. Section III shows the control diagram of the proposed method. Section IV shows the simulation and experiment result of proposed control method.

II. THE DERIVATION OF DUALITY DROOP CONTROL FOR CASCADED MICROINVERTER SYSTEM

For traditional parallel inverter system which is shown on the right side of figure.1, the active power and reactive power are controlled by its angle and amplitude respectively which can be summarized as equation (1). This control law is usually adopted in parallel inverter system.

$$\begin{cases}
P_n \propto \varphi_n \\
Q_n \propto (V_n - V_{out})
\end{cases} \quad n \in \{1, 2, 3\}$$
(1)

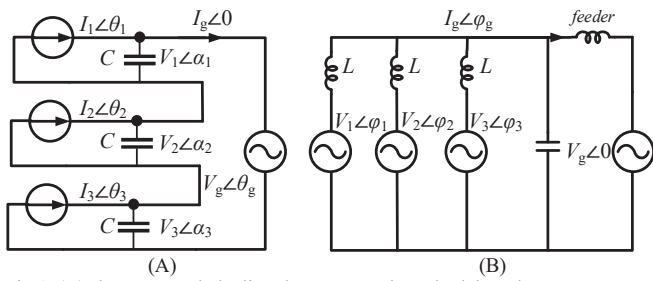


Fig.1 (A)The proposed duality droop control method based current-source structure for cascaded microinverter system (B) The traditional droop control method-based voltage-source structure for parallel microinverter system

For the cascaded microinverter system which is shown on the left-hand side of Fig. 1, one method that is duality to parallel inverter system can be derived based on droop control law. The capacitor voltage of each submodule can be expressed as equation (2). As can be seen in the Fig. 1(A), the feeder inductor between power grid and inverter system are removed.

$$v_{c(n)} = \frac{\left(l_n e^{j\theta_n} - l_g\right)}{j\omega c}$$

$$= \left[\frac{l_n \sin(\theta_n)}{\omega c}\right] + j\left[\frac{l_g - l_n \cos(\theta_n)}{\omega c}\right] \quad n \in \{1,2,3\}$$
Then the complex power of each submodule can be

Then the complex power of each submodule can be expressed as equation (3). It should be noted that the angle θ_n is very small because the current that flows through the capacitor is very small.

$$S = v_{c(n)} \times i_{(n)}^{*}$$

$$= \left\{ \begin{bmatrix} I_{n} \sin(\theta_{n}) \\ \omega C \end{bmatrix} + j \begin{bmatrix} I_{g} - I_{n} \cos(\theta_{n}) \\ \omega C \end{bmatrix} \right\}$$

$$\times \left\{ I_{n} \cos(\theta_{n}) - j I_{n} \sin(\theta_{n}) \right\}$$

$$= \frac{I_{g} I_{n} \sin(\theta_{n})}{\omega C} + j \frac{I_{n} \left(I_{g} \cos(\theta_{n}) - I_{n} \right)}{\omega C}$$

$$\approx \frac{I_{g} I_{n} \theta_{n}}{\omega C} + j \frac{I_{n} \left(I_{g} - I_{n} \right)}{\omega C}$$

$$= P_{n} + j Q_{n}$$
(3)

According to the derivation from equation (3), if $I_{\rm g}$ is constant, the active and reactive power of the cascaded microinverter systems is proportional to $\theta_{\rm n}$ and $(I_{\rm g}\text{-}I_{\rm n})$ respectively, which can be expressed in equation (4). Compared with the equation (1) of the traditional droop control, the proposed control method which is adopted in the cascaded microinverter system is with duality to it. Moreover, it should be noted that the sign of $I_{\rm n}$ is negative, therefore the line of current amplitude versa reactive power should be tilted up which is shown fig.2. Therefore, for grid-tied connected microinverter system,

$$\begin{cases}
P_n \propto \theta_n \\
Q_n \propto (I_g - I_n)
\end{cases}$$
(4)

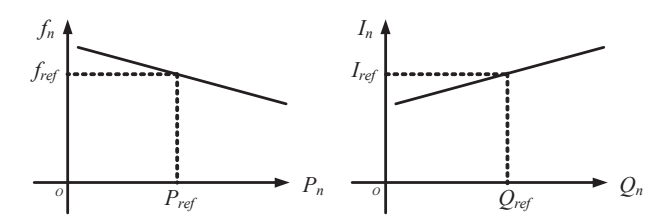


Fig. 2 The droop control law for cascaded microinverter system.

$$\sum_{N} v_{c(n)} = v_g \tag{5}$$

$$I_g = \frac{\sum_n I_n e^{j\theta_n} - j\omega c v_g}{3} \approx \frac{\sum_n I_n e^{j\theta_n}}{3} \tag{6}$$

Fig. 2 The droop control law for cascaded microinverter system.
$$\sum_{N} v_{c(n)} = v_{g}$$
 (5)
$$I_{g} = \frac{\sum_{n} I_{n} e^{j\theta_{n}} - j\omega c v_{g}}{3} \approx \frac{\sum_{n} I_{n} e^{j\theta_{n}}}{3}$$
 (6)
$$S_{g} = \frac{\sum_{n} I_{n} e^{j(-\theta_{n})}}{3} V_{g} e^{j\theta_{g}} = \frac{\sum_{n} V_{g} I_{n} e^{j(\theta_{g} - \theta_{n})}}{3}$$
 (7)
$$= \frac{\sum_{n} V_{g} I_{n} \cos(\theta_{g} - \theta_{n})}{3} + j \frac{\sum_{n} V_{g} I_{n} \sin(\theta_{g} - \theta_{n})}{3}$$
 (8)
$$\begin{cases} P_{g} \propto I_{n} \\ Q_{n} \propto \sin(\theta_{g} - \theta_{n}) \approx (\theta_{g} - \theta_{n}) \end{cases}$$
 Moreover, according to equation (2), equation (6) can be derived. Then the complex power that injects to power grid can

derived. Then the complex power that injects to power grid can be expressed as equation (7). It can be found that the active power is proportional to the active power and reactive power is proportional to the $(\theta_g - \theta_n)$. Therefore, by adjusting all submodules' reference current amplitude simultaneously, the active power can be adjusted. Moreover, by adjusting all submodules' angle phase simultaneously, the reactive power can be adjusted. Therefore, for central control unit, the control algorithm is shown in Fig.3.

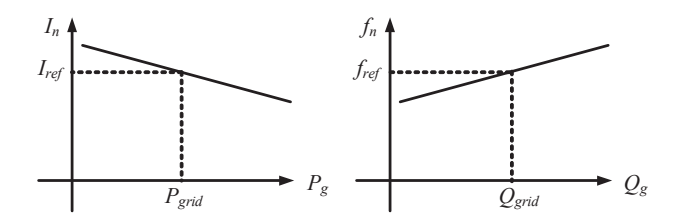


Fig. 3 The control algorithm of the central unit

THE COMPARISON BETWEEN INVERSED DROOP CONTROL AND THE PROPOSED CONTROL LAW

Fig. 4 shows one of the control methods which is based on the inverse droop control^[22]. It's consisted of three stages which are boost stage, LLC stage and inverter stage respectively. The boost stage adapts primary side voltage as outer loop feedback variable and inductor current as inner loop feedback variable. The LLC circuit feedbacks secondary side voltage to adjust the PWM frequency.

Regarding to the inverter stage, the reactive power is calculated by sampling each submodule's output voltage and current. Then the output active power and reactive power can be calculated respectively. After that, the inverse droop controlmethod based algorithm that adjusts each submodule frequency according to its reactive power is adopted.

Different from the previous control method, the proposed duality control method under island mode in this paper is shown in Fig. 5. For the boost stage and LLC stage of every submodule, the control method is the same. For the inverter

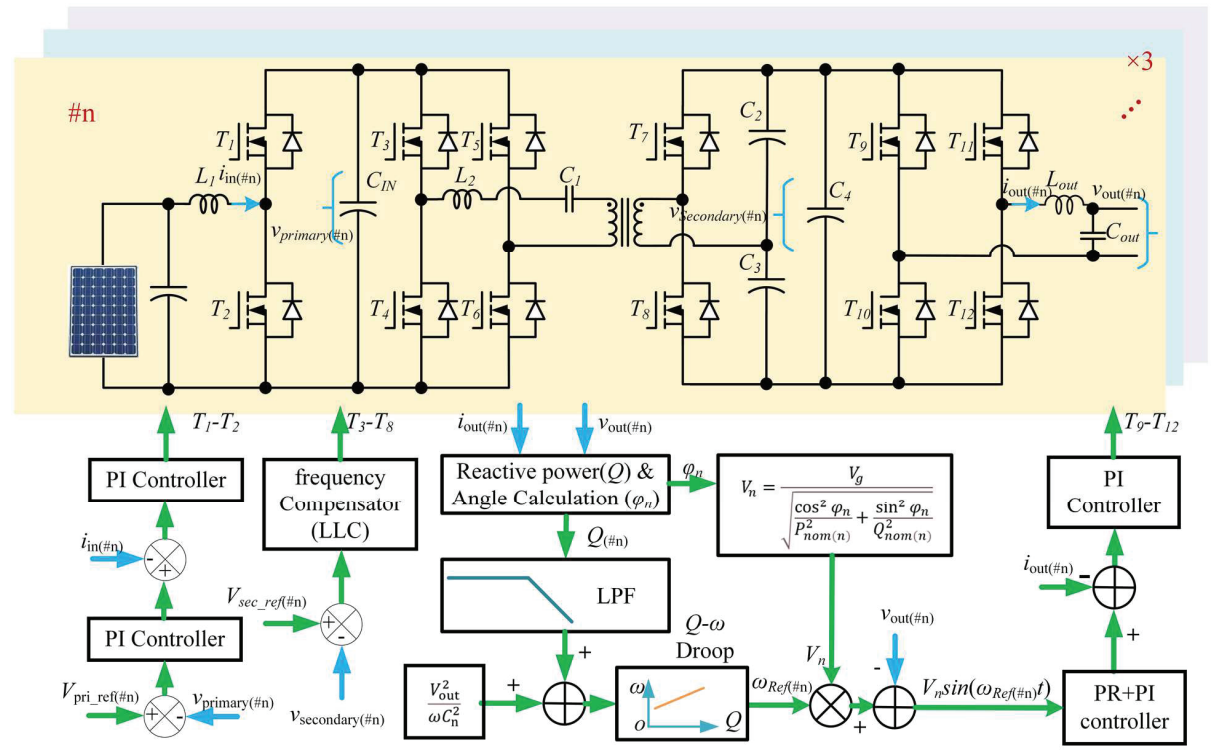


Fig. 4 Fully decoupled active and reactive power control for CCM system.

stage, the output current and voltage are sampled and filtered out by the low pass filter. Then the reference current amplitude I_n is adjusted according to each submodule's reactive power and the frequency f_n is also adjusted by each submodule's active power. After the reference current is generated, then a typical PI controller is adopted to control submodule's output current.

If the two control methods shown in Fig. 4 and Fig. 5 are compared, it can be found that there are two droop control line in Fig. 5 while there is just one droop control line in Fig. 4. This means the control law shown in Fig. 5 can control two degrees of freedom simultaneously. Moreover, the method shown in Fig. 5 makes the microinverter works as current source inverter while the method shown in Fig. 4 makes the microinverter works as voltage source inverter. Therefore, this is the reason why the feeder inductor between power grid and microinverter system can be removed.

Based on the duality droop control method for island mode, the grid-tied duality control method is shown in Fig. 8. For the central control unit, the $\Delta I_{\rm g}$ and $\Delta \omega_{\rm g}$ are calculated respectively according to $P_{\rm g}$ and $Q_{\rm g}$. Then the generated $\Delta I_{\rm g}$ and $\Delta \omega_{\rm g}$ are sent to all the local controllers for the desired total active power and reactive power injected to power grid. Generally speaking, the proposed duality droop control for the local controller is to guarantee the power is averagely distributed among all the submodules, while the central control unit is to ensure the desired active and reactive power injected to the power grid. In order to transmit the $\Delta I_{\rm g}$ and $\Delta \omega_{\rm g}$ to local controller, therefore the communication part is needed within the local control units and the central control unit.

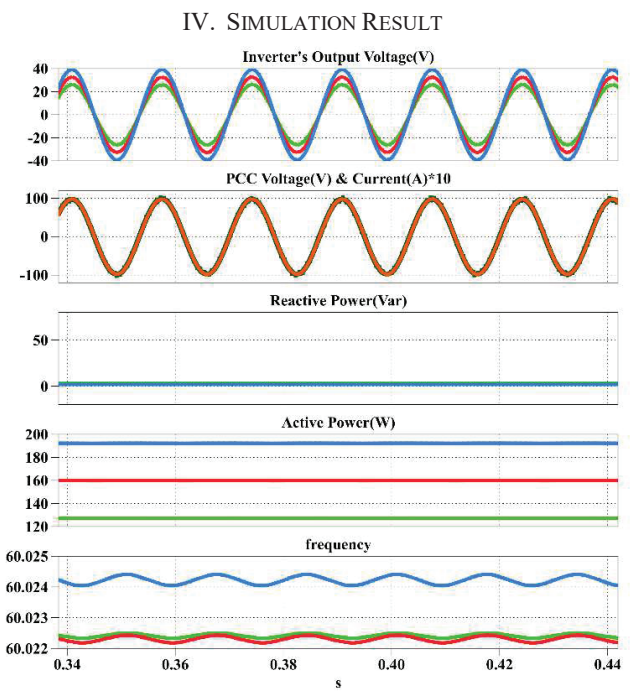


Fig. 6 The simulation result when the CCM system is with the duality control method shown in Fig. 5

The simulation result shown in Fig. 6 is in island mode with duality control, the PCC voltage is set as 100V/60Hz, and the active power ratio is set as 1.2:1:0.8, while the reactive power ratio is set as 1.2:1:0.8.

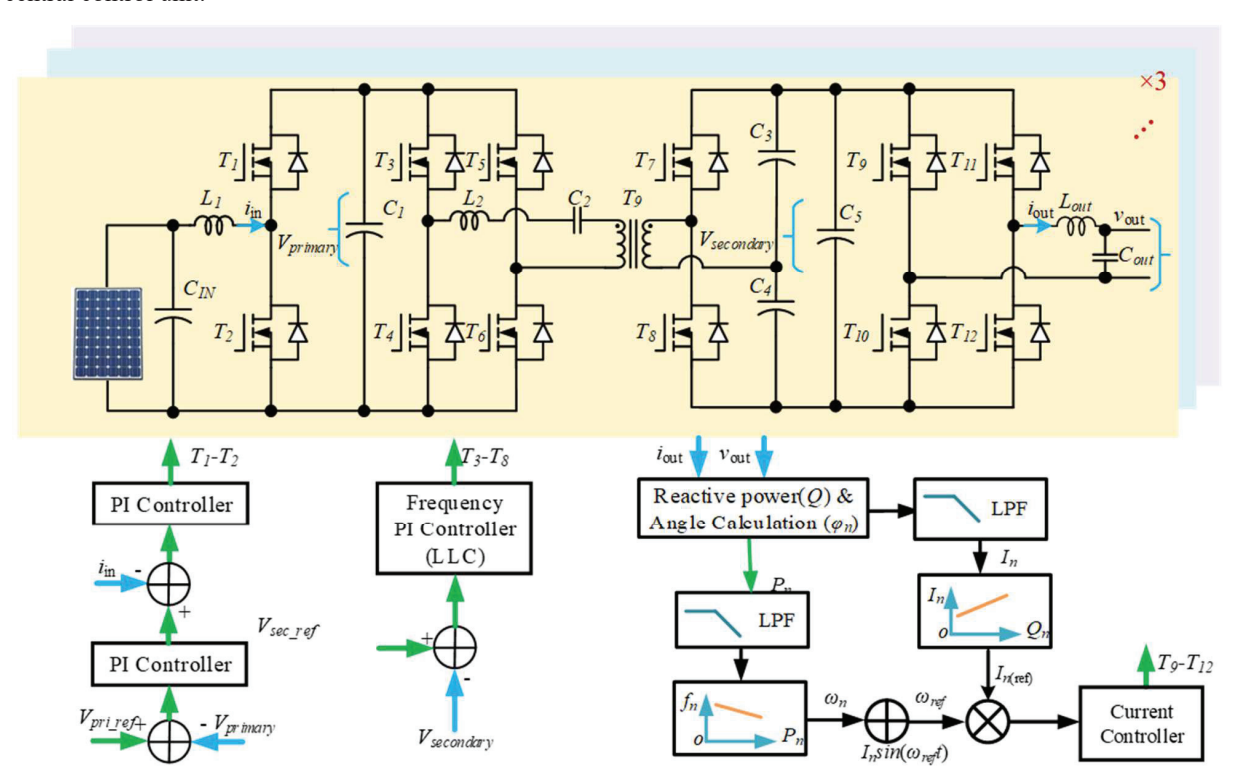


Fig. 5 The proposed duality control method for island microinverter system

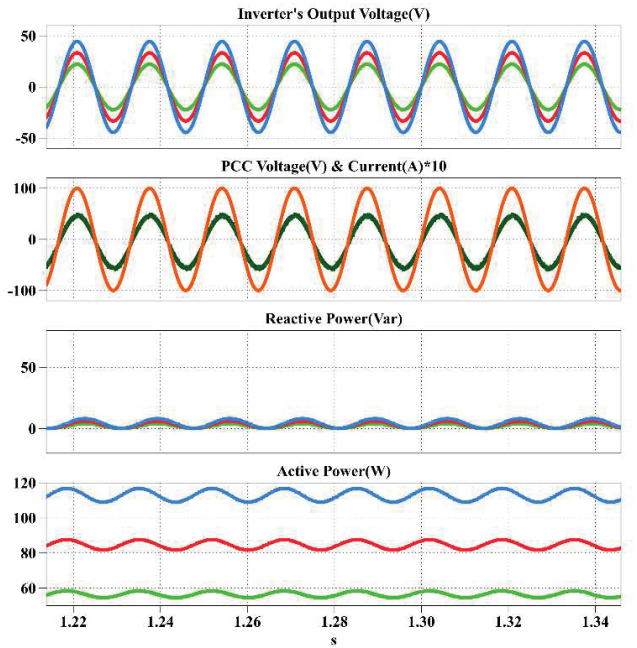


Fig. 7 The simulation result when the CCM system is with the duality control method shown in Fig. 8

The simulation result shown in Fig. 7 is in grid-tied mode with duality control, the grid voltage is set as 100V/60Hz, and the active power ratio is set as 1.2:1:0.8, while the reactive power ratio is set as 1:1:1. From the simulation result, it proves the feasibility of the proposed control method.

V. EXPERIMENTAL RESULT

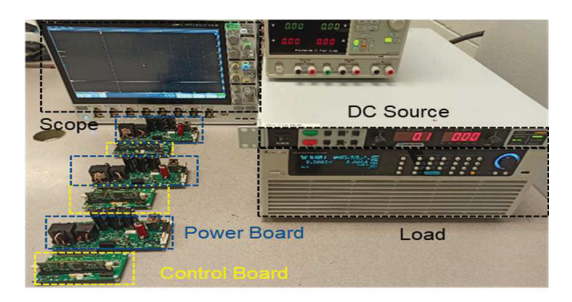


Fig. 9 The prototype of three microinverters in cascaded

Fig. 9 shows the experimental setup of three submodules in cascaded. Each submodule is constituted by a power board and a control board. The calculation task is finished by DSP28335.

Fig. 10 shows the experimental result under island mode with the inverse droop control based method shown in Fig. 4, and the active power of three submodules is set as 1.2:1:0.8, and the PCC voltage is set as 100V/60Hz. Blue, red and black waveforms are the output voltage of the three converters, and the orange yellow waveform is the PCC voltage current. Fig. 11 shows the shows the experimental result with duality control shown in Fig. 5, and the active power of three modules is set as 1.2:1:0.8 under island mode. The PCC voltage is set as 100V/60Hz. Blue, red and black waveforms are the output voltage of the three converters, and the orange yellow waveform is the PCC voltage current. Both the results shown in Fig. 9 and Fig. 10 are very close to each other.

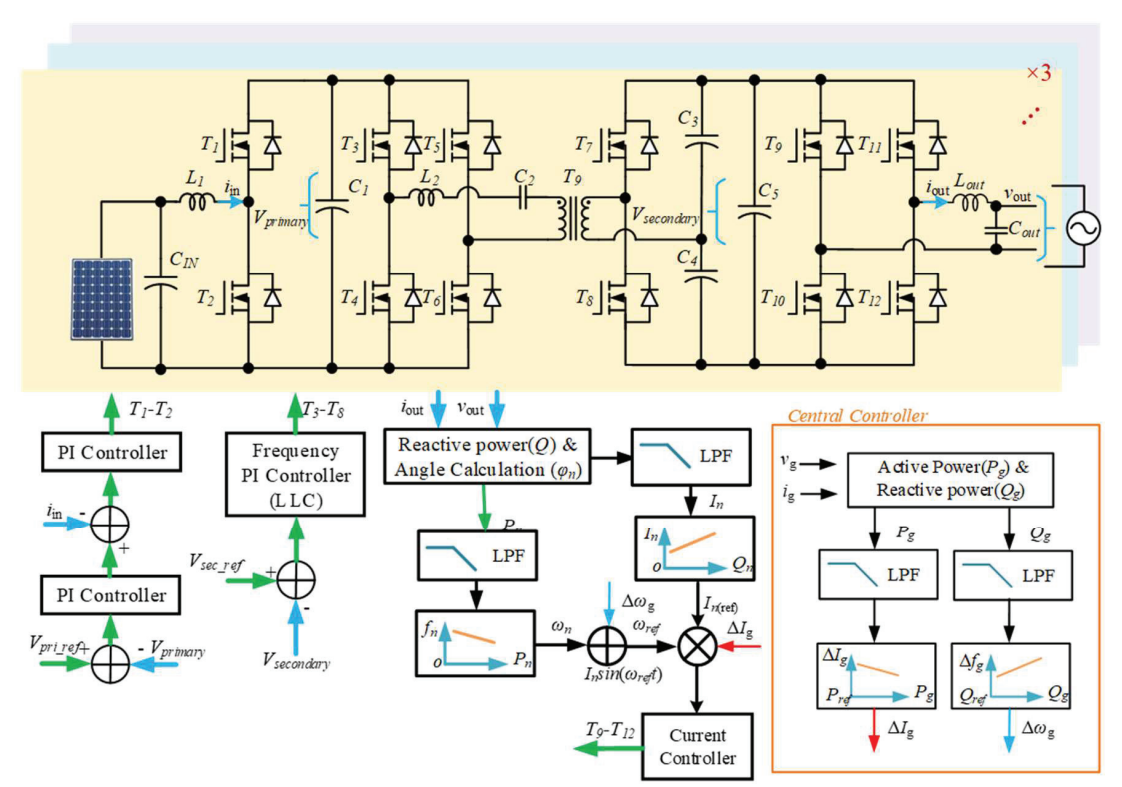


Fig. 8 The proposed duality control method for grid-tied microinverter system

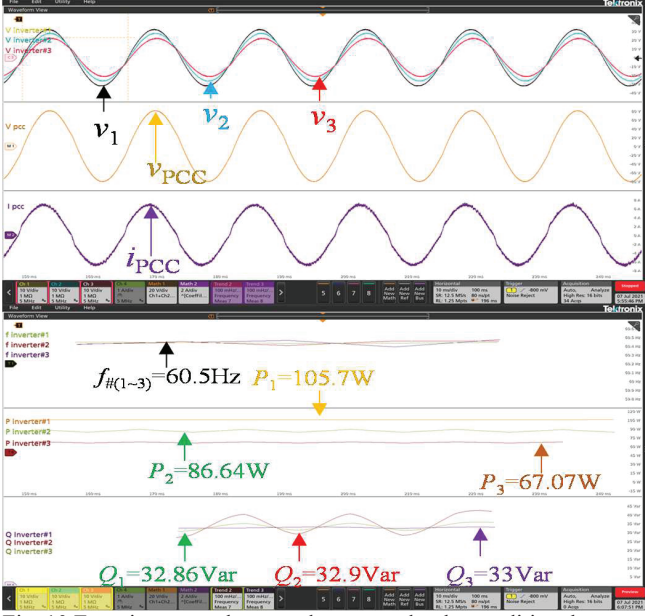


Fig. 10 Experiment result at steady state under the condition that $P_1:P_2:P_3=1.2:1:0.8 \& Q_1:Q_2:Q_3=1:1:1$

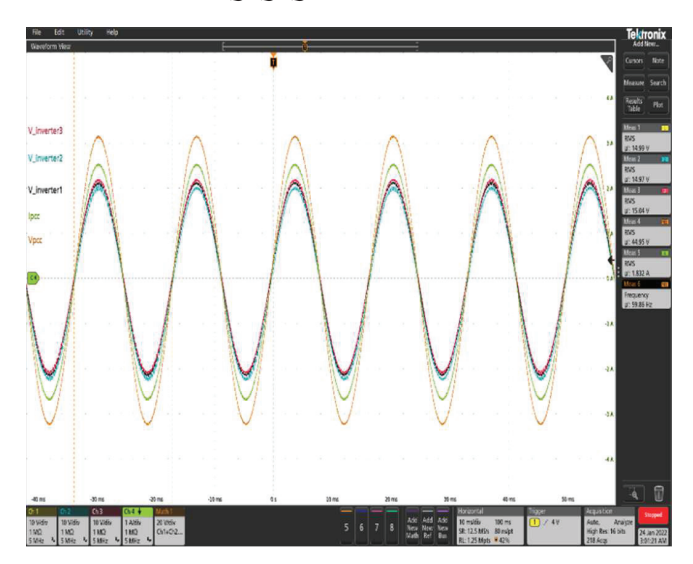


Fig. 11 The experimental result when three microinverter in cascaded

VI. CONCLUSIONS

This paper proposes a new duality droop control method which is suitable for cascaded inverter system. By this method, every inverter submodule works as current source inverter, and the feeder inductor can be removed under grid tied mode. Moreover, the inverse droop control method and the proposed duality control method are compared in the experimental result. The simulation result proves the feasibility of the proposed control method under both island and grid-tie mode. The experiment result proves the proposed control method is feasible under island mode. In the future, the grid-tied experimental will be conducted.

REFERENCES

- [1] S. Kouro, J. I. Leon, D. Vinnikov and L. G. Franquelo, "Grid-Connected Photovoltaic Systems: An Overview of Recent Research and Emerging PV Converter Technology," in IEEE Industrial Electronics Magazine, vol. 9, no. 1, pp. 47-61, March 2015, doi: 10.1109/MIE.2014.2376976.
- [2] A. I. Elsanabary, G. Konstantinou, S. Mekhilef, C. D. Townsend, M. Seyedmahmoudian and A. Stojcevski, "Medium Voltage Large-Scale Grid-Connected Photovoltaic Systems Using Cascaded H-Bridge and Modular Multilevel Converters: A Review," in IEEE Access, vol. 8, pp. 223686-223699, 2020, doi: 10.1109/ACCESS.2020.3044882.
- [3] H. Akagi, "Classification, Terminology, and Application of the Modular Multilevel Cascade Converter (MMCC)," in IEEE Transactions on Power Electronics, vol. 26, no. 11, pp. 3119-3130, Nov. 2011, doi: 10.1109/TPEL.2011.2143431.
- [4] Jih-Sheng Lai and Fang Zheng Peng, "Multilevel converters-a new breed of power converters," in IEEE Transactions on Industry Applications, vol. 32, no. 3, pp. 509-517, May-June 1996, doi: 10.1109/28.502161.
- [5] S. Yang, Y. Liu, X. Wang, D. Gunasekaran, U. Karki and F. Z. Peng, "Modulation and Control of Transformerless UPFC," in IEEE Transactions on Power Electronics, vol. 31, no. 2, pp. 1050-1063, Feb. 2016, doi: 10.1109/TPEL.2015.2416331.
- [6] Y. Li, X. Lyu, D. Cao, S. Jiang and C. Nan, "A 98.55% Efficiency Switched-Tank Converter for Data Center Application," in IEEE Transactions on Industry Applications, vol. 54, no. 6, pp. 6205-6222, Nov.-Dec. 2018, doi: 10.1109/TIA.2018.2858741.
- [7] Z. Ni, S. Zheng, M. S. Chinthavali and D. Cao, "Investigation of Dynamic Temperature-Sensitive Electrical Parameters for Medium-Voltage Low-Current Silicon Carbide and Silicon Devices," 2020 IEEE Energy Conversion Congress and Exposition (ECCE), 2020, pp. 3376-3382, doi: 10.1109/ECCE44975.2020.9236121.
- [8] C. B. Barth et al., "Design and control of a GaN-based, 13-level, flying capacitor multilevel inverter," 2016 IEEE 17th Workshop on Control and Modeling for Power Electronics (COMPEL), 2016, pp. 1-6, doi: 10.1109/COMPEL.2016.7556770.
- [9] A. Lidow, J. Strydom, R. Strittmatter and C. Zhou, "GaN: A Reliable Future in Power Conversion: Dramatic performance improvements at a lower cost," in IEEE Power Electronics Magazine, vol. 2, no. 1, pp. 20-26, March 2015, doi: 10.1109/MPEL.2014.2381457.
- [10] T. Fang, S. Shen, Y. Jin, X. Zhang, Z. Han and X. Ruan, "Multiple-Objective Control Scheme for Input-Series—Output-Series LCL-Filtered Grid-Connected Inverter System," in IEEE Transactions on Power Electronics, vol. 35, no. 8, pp. 8689-8700, Aug. 2020, doi: 10.1109/TPEL.2020.2964112.
- [11] B. P. McGrath, D. G. Holmes and W. Y. Kong, "A Decentralized Controller Architecture for a Cascaded H-Bridge Multilevel Converter," in IEEE Transactions on Industrial Electronics, vol. 61, no. 3, pp. 1169-1178, March 2014, doi: 10.1109/TIE.2013.2261032.
- [12] J. He, Y. Li, B. Liang and C. Wang, "Inverse Power Factor Droop Control for Decentralized Power Shari Ing in Series-Connected-Microconverters-Based Islanding Microgrids," in IEEE Transactions on Industrial Electronics, vol. 64, no. 9, pp. 7444-7454, Sept. 2017, doi: 10.1109/TIE.2017.2674588.
- [13] H. Jafarian, R. Cox, J. H. Enslin, S. Bhowmik and B. Parkhideh, "Decentralized Active and Reactive Power Control for an AC-Stacked PV Inverter With Single Member Phase Compensation," in IEEE Transactions on Industry Applications, vol. 54, no. 1, pp. 345-355, Jan.-Feb. 2018, doi: 10.1109/TIA.2017.2761831.
- [14] L. Zhang, K. Sun, Z. Huang and Y. W. Li, "A grid-tied photovoltaic generation system based on series-connected module integrated inverters with adjustable power factor," 2015 IEEE Energy Conversion Congress and Exposition (ECCE), 2015, pp. 6864-6870, doi: 10.1109/ECCE.2015.7310621.
- [15] M. Wang et al., "Harmonic Compensation Strategy for Single-Phase Cascaded H-Bridge PV Inverter Under Unbalanced Power Conditions," in IEEE Transactions on Industrial Electronics, vol. 67, no. 12, pp. 10474-10484, Dec. 2020, doi: 10.1109/TIE.2019.2962461.
- [16] Z. Ma, S. Wang, H. Sheng and S. Lakshmikanthan, "Modeling, Analysis and Mitigation of Radiated EMI due to PCB Ground Impedance in a 65W High-density Active-clamp Flyback Converter," in IEEE Transactions on Industrial Electronics, Early access.

- [17] P. Liu, L. Song and S. Duan, "A Synchronization Method for the Modular Series-Connected Inverters," in IEEE Transactions on Power Electronics, vol. 35, no. 7, pp. 6686-6690, July 2020, doi: 10.1109/TPEL.2019.2961397.
- [18] Z. Ma, Y. Li, S. Wang, H. Sheng and S. Lakshmikanthan, "Investigation and Reduction of EMI Noise Due to the Reverse Recovery Currents of 50/60 Hz Diode Rectifiers," in IEEE Journal of Emerging and Selected Topics in Industrial Electronics, vol. 3, no. 3, pp. 594-603, July 2022.
- [19] L. Zhang, K. Sun, Y. W. Li, X. Lu and J. Zhao, "A Distributed Power Control of Series-Connected Module-Integrated Inverters for PV Grid-Tied Applications," in IEEE Transactions on Power Electronics, vol. 33, no. 9, pp. 7698-7707, Sept. 2018, doi: 10.1109/TPEL.2017.2769487.
- [20] X. Hou and K. Sun, "An Improved Decentralized Control of Grid-Connected Cascaded Inverters with Different Power Capacities," 2021

- IEEE 12th International Symposium on Power Electronics for Distributed Generation Systems (PEDG), 2021, pp. 1-5, doi: 10.1109/PEDG51384.2021.9494264.
- [21] Z. Ma and S. Wang, "Prediction and Measurement Techniques for Radiated EMI of Power Converters with Cables," in Chinese Journal of Electrical Engineering.
- [22] M. Qiu, M. Wei, S. Yang, X. Liu and D. Cao, "Active and Reactive Power Distribution for Cascaded-H-Bridge Microinverters under Island Microgrid," 2021 IEEE Energy Conversion Congress and Exposition (ECCE), 2021, pp. 777-782, doi: 10.1109/ECCE47101.2021.9595590.